JCTC Journal of Chemical Theory and Computation

Article

pubs.acs.org/JCTC

Excited State Absorption from Real-Time Time-Dependent Density Functional Theory

Sean A. Fischer,[†] Christopher J. Cramer,[‡] and Niranjan Govind*[,†]

[†]Environmental Molecular Sciences Laboratory, Pacific Northwest National Laboratory, P.O. Box 999, Richland, Washington 99352, United States

[‡]Department of Chemistry, Supercomputing Institute and Chemical Theory Center, University of Minnesota, Minneapolis, Minnesota 55455, United States

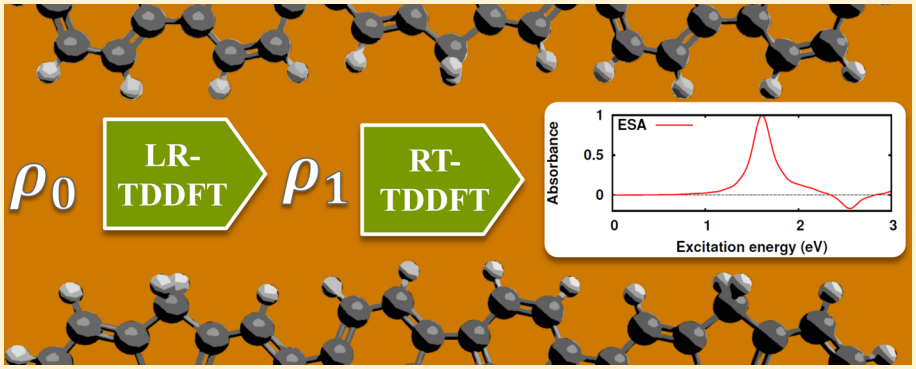

ABSTRACT: The optical response of excited states is a key property used to probe photophysical and photochemical dynamics. Additionally, materials with a large nonlinear absorption cross-section caused by two-photon (TPA) and excited state absorption (ESA) are desirable for optical limiting applications. The ability to predict the optical response of excited states would help in the interpretation of transient absorption experiments and aid in the search for and design of optical limiting materials. We have developed an approach to obtain excited state absorption spectra by combining real-time (RT) and linear-response (LR) time-dependent density functional theory (TDDFT). Being based on RT-TDDFT, our method is aimed at tackling larger molecular complexes and materials systems where excited state absorption is predominantly seen and many time-resolved experimental efforts are focused. To demonstrate our method, we have calculated the ground and excited state spectra of H_2^+ and H_2 due to the simplicity in the interpretation of the spectra. We have validated our new approach by comparing our results for butadiene with previously published results based on quadratic response (QR). We also present results for oligofluorenes, where we compare our results with both QR-TDDFT and experimental measurements. Because our method directly measures the response of an excited state, stimulated emission features are also captured; although, these features are underestimated in energy which could be attributed to a change of the reference from the ground to the excited state.

1. INTRODUCTION

Transient absorption spectroscopy is used to probe the dynamics of excited states.[1] Due to overlapping features and difficulties in assigning lifetimes of excited states, the interpretation of these time-resolved experiments is challenging. The ability to simulate excited state dynamics can greatly aid in the interpretation of the experimental results.[2] Invariably the question arises as to the accuracy of the simulation with respect to the experiment, especially for large systems where more approximations are required for the electronic structure theory and nuclear dynamics. A convenient benchmark for the simulation would be the prediction of the experimental observable. In the case of transient absorption spectroscopy, that means the ability to calculate the excited state absorption (ESA) of systems. Additionally, the reliable prediction of ESA could be used to find and optimize materials for optical limiting applications.[3,4]

Response theory is currently the primary method through which ESA is obtained.[5,6] The poles of the linear response (LR) function give the excitation energies of the system, while the second order residues of the quadratic response (QR) function are used to obtain transition moments between two non-reference states. As the ground state is by far the most common reference state for response calculations, the QR of the ground state can be used to obtain the ESA spectrum of a molecule. Alternatively, LR with one of the excited states as the reference can also be used. Both these approaches are identical for the exact theory (for example, full CI[5]), but this is not the case for approximate methods. Advantages of QR are that only the ground state needs to be optimized and it is possible to obtain two-photon absorption (first order residues of the QR

Received: May 21, 2015
Published: August 13, 2015

DOI: 10.1021/acs.jctc.5b00473
J. Chem. Theory Comput. 2015, 11, 4294−4303

function) at the same time. However, ESA is typically seen most prominently in large molecular and materials systems. Problematic for QR is the high density of states that is associated with these systems. With QR each root must be solved for individually, which can quickly become prohibitive if a complete spectrum is needed.

For the ground-state absorption of large systems real-time, time-dependent density functional theory (RT-TDDFT) is an efficient approach for obtaining the spectrum[7,8] and would be an attractive alternative to QR-TDDFT if extended to ESA. De Giovannini et al.[9] have proposed a simulation protocol based on RT-TDDFT that is a direct simulation of a pump/probe experiment. One electric field is applied to excite the system to the state of interest, and then a second field is used to probe the response of the excited density. This approach is intuitively appealing and only requires the explicit optimization of the ground state. However, with this procedure there is a question as to whether the correct state is being probed since resonant excitations within RT-TDDFT have been shown to be problematic,[9−16] and the greatest possible overlap with a singly excited state from a closed-shell ground state is 50%.[17]

Our new approach avoids the current ambiguities with resonant excitations in the context of RT-TDDFT but still uses RT-TDDFT to obtain the response of the excited state. We accomplish this by using the excited-state density calculated using LR-TDDFT gradients as the starting density for a RT-TDDFT propagation. In this manner, we calculate the linear response of the excited state of interest, rather than the quadratic response of the ground state. Li and co-workers have previously performed RT-TDDFT and Ehrenfest simulations starting from a LR-TDDFT excited-state density to investigate the lifetime of the excited state;[18,19] although, they did not consider the response of the excited state to an applied electric field. The present work does just that and gives full consideration to the effects of employing approximations to the exchange-correlation kernels. A simple procedure for overcoming one of the difficulties associated with determining the response of the excited-state density to an applied electric field using these approximations is also outlined.

In the next section, we give the details of our method and explain the caveats that come with the use of currently available approximations to the exchange-correlation kernels. We then take a minor detour to show the remarkable ability of RT-TDDFT to obtain an accurate absorption spectrum from an unconverged density and explain how this ability lends credibility to our ESA calculations. As a first test of our approach we compare our results for the ESA spectrum of butadiene to previously published results based on quadratic response theory. We then move to larger molecules, a pair of oligofluorenes, where we compare our results with both quadratic response and experimental measurements. We conclude with an outlook of our approach and its potential role in the development of new exchange-correlation kernels.

2. METHODS

As stated above, our new approach to obtain the ESA is to calculate the linear response of an excited state of interest. This is accomplished by using the excited-state density obtained from LR-TDDFT gradients[20,21] as the starting point for a RT-TDDFT calculation. Within an exact electronic structure theory, the linear response of the excited state will provide identical information to the quadratic response of the ground state.[5] Formally, the LR-TDDFT excited-state density is the exact density of the excited state. Similarly, the RT-TDDFT propagation of the excited state density is formally exact. However, in both cases, the exact exchange-correlation kernels are unknown and approximations must be made.

While the exact exchange-correlation kernel is a functional of the initial state and full history of the density, all widely used approximations are simply functionals of the instantaneous density.[22] Elliott and Maitra have examined the errors associated with both this adiabatic approximation and approximate exchange-correlation functionals on the propagation of initially excited states.[23] For their model two and four electron systems they found that the errors can be substantial and depend on the choice of the initial Kohn−Sham state: the best results are those for which the Kohn−Sham state has a configuration most similar to the true, interacting state. In our scheme we never explicitly construct a Kohn−Sham wave function; we work entirely with density matrices. Formally, this would pose a difficulty since the exact exchange-correlation kernel would be a functional of the initial Kohn−Sham state; however, since we exclusively make use of the adiabatic approximation, there is no initial state dependence in the exchange-correlation kernels that we use in the calculations. If initial-state-dependent kernels were developed, then a possible ansatz to construct an initial Kohn−Sham state would be to project the excited state density on to the space of the ground state molecular orbitals. A Kohn−Sham wave function with potentially fractionally occupied molecular orbitals could then be constructed. These occupations would be similar to those derived from the squares of the coefficients of the LR-TDDFT transition vectors, e.g. for an excitation dominated by a transition between a single pair of molecular orbitals, the populations of those orbitals would be close to 1 while the populations of the remaining orbitals would be close to 0 or 2.

The time-dependent Kohn−Sham equations as initially formulated by Runge and Gross[24] were derived for an idempotent density matrix. In general the density matrix produced from a LR-TDDFT gradients calculation will not be idempotent (see the Appendix for details); however, this presents no difficulties as the Runge-Gross theorem has been extended to include arbitrary ensembles.[25,26] In fact van Leeuwen has shown that the only conditions the noninteracting system must satisfy in order to reproduce the density of the interacting system are that the initial density and time derivative of the density must match the interacting system.[27] Therefore, in contrast to time-independent DFT, the initial noninteracting system in TDDFT does not have to be representable by a single Slater determinant (i.e., an idempotent density).

An additional subtlety arises when approximations are used for the exchange-correlation kernels. The ground-state density is used in the construction of the electronic potential for the calculation of the excited-state density with LR-TDDFT. When we begin to propagate that excited-state density, the excited-state density is now used in the construction of the electronic potential. Upon going from calculating the excited-state density with LR-TDDFT to propagating the excited-state density with RT-TDDFT, we have changed our reference state from the ground state to the excited state. One effect of this will be transition frequencies from the excited state that do not necessarily agree with those from the ground state. As Isborn and Li demonstrated for TDDFT[28] and Constrand et al. demonstrated with complete active space self-consistent field wave functions,[5] the response frequencies of the system depend on the reference state for approximate methods. This is an

DOI: 10.1021/acs.jctc.5b00473
J. Chem. Theory Comput. 2015, 11, 4294−4303

unsolved problem for the simulation of resonant excitations in RT-TDDFT.[9−16]

This change of reference leads to another complication. When RT-TDDFT is used to calculate the ground state optical absorption spectrum of a molecule, the initial state is a stationary state; therefore, the only dynamics during the propagation are due to the applied electric field. When initially calculated, our LR-TDDFT excited state is stationary as well. However, that is only true as long as the ground state is our reference state. As mentioned previously, when we propagate the excited-state density with RT-TDDFT, the excited state is now our reference state. This leads to a nonstationary initial density matrix, even before an electric field is applied. This may seem problematic in light of van Leeuwen's condition on the initial time derivative of the density stated above. However, it is straightforward to show that as long as the initial density matrix and Fock matrix of the noninteracting system are purely real, then the initial time derivative of the density will also be zero: If the initial density matrix and Fock matrix are purely real, then the initial time derivative of the density matrix (if nonzero) will be purely imaginary. Since the basis functions are time-independent and the density only depends on the real part of the density matrix,[29] then the initial time derivative of the density will be zero. In order to be able to extract a meaningful response from the system though, we need to account for the initial density matrix not being stationary. We accomplish this by making use of a moving reference. This bears similarities to the work of De Giovannini et al. where they simulated a pump/probe experiment and tracked the response of the dipole to the probe pulse relative to the response of the dipole to the pump pulse.[9]

We begin with the time-dependent Kohn−Sham equation, cast in terms of the single-particle reduced density matrix

$$i\frac{\partial \mathbf{P}'(t)}{\partial t} = [\mathbf{F}'(t), \mathbf{P}'(t)] \tag{1}$$

where $\mathbf{F}'(t)$ is the Fock matrix. The prime indicates that we are in an orthonormal basis. If our initial density matrix is nonstationary and we are interested in the response to an electric field, we need to be able to separate the dynamics due to being away from a stationary point and those due to the electric field. Assuming that our initial state is not far from the stationary point, we can rewrite our density matrix, to first order, as

$$\mathbf{P}'(t) = \mathbf{P}'(0) + \delta\mathbf{P}'_{NS}(t) + \delta\mathbf{P}'_{EF}(t) \tag{2a}$$

which implies an analogous separation of the Fock matrix

$$\mathbf{F}'(t) = \mathbf{F}'(0) + \delta\mathbf{F}'_{NS}(t) + \delta\mathbf{F}'_{EF}(t) \tag{2b}$$

where $\mathbf{P}'(0)$ represents the static density matrix, $\delta\mathbf{P}'_{NS}(t)$ represents the deviation of our initial density matrix from the stationary one, and $\delta\mathbf{P}'_{EF}(t)$ represents the perturbation caused by the electric field. The Fock matrices are defined analogously.

Substitution of eqs 2a and 2b into eq 1 yields

$$\begin{aligned} I\frac{\partial \delta\mathbf{P}'_{NS}(t)}{\partial t} + i\frac{\partial \delta\mathbf{P}'_{EF}(t)}{\partial t} &= [\mathbf{F}'(0), \delta\mathbf{P}'_{NS}(t)] + [\mathbf{F}'(0), \delta\mathbf{P}'_{EF}(t)] \\ &+ [\delta\mathbf{F}'_{NS}(t), \mathbf{P}'(0)] + [\delta\mathbf{F}'_{EF}(t), \mathbf{P}'(0)] \\ &+ [\delta\mathbf{F}'_{NS}(t), \delta\mathbf{P}'_{EF}(t)] + [\delta\mathbf{F}'_{NS}(t), \delta\mathbf{P}'_{NS}(t)] \\ &+ [\delta\mathbf{F}'_{EF}(t), \delta\mathbf{P}'_{NS}(t)] + [\delta\mathbf{F}'_{EF}(t), \delta\mathbf{P}'_{EF}(t)] \end{aligned} \tag{3}$$

where we have used the fact that $\mathbf{P}'(0)$ is time-independent and commutes with the static Fock matrix. If we now only consider terms that are linear with respect to perturbation away from the static density matrix eq 3 becomes

$$\begin{aligned} i\frac{\partial \delta\mathbf{P}'_{NS}(t)}{\partial t} + i\frac{\partial \delta\mathbf{P}'_{EF}(t)}{\partial t} &= [\mathbf{F}'(0), \delta\mathbf{P}'_{NS}(t)] + [\mathbf{F}'(0), \delta\mathbf{P}'_{EF}(t)] \\ &+ [\delta\mathbf{F}'_{NS}(t), \mathbf{P}'(0)] + [\delta\mathbf{F}'_{EF}(t), \mathbf{P}'(0)] \end{aligned} \tag{4}$$

which can be separated into an equation for the response due to the applied field and an equation for the response due to being away from the stationary density matrix:

$$i\frac{\partial \delta\mathbf{P}'_{EF}(t)}{\partial t} = [\mathbf{F}'(0), \delta\mathbf{P}'_{EF}(t)] + [\delta\mathbf{F}'_{EF}(t), \mathbf{P}'(0)] \tag{5}$$

$$i\frac{\partial \delta\mathbf{P}'_{NS}(t)}{\partial t} = [\mathbf{F}'(0), \delta\mathbf{P}'_{NS}(t)] + [\delta\mathbf{F}'_{NS}(t), \mathbf{P}'(0)] \tag{6}$$

These equations suggest a simple procedure to account for the nonstationary starting density matrix. First, the system is propagated under the influence of the applied electric field. The response of the system includes both the dynamics due to the electric field and the dynamics due to the nonstationary initial state. Next, the system is propagated without an applied field. The response of the system this time only includes the dynamics due to the nonstationary initial state, thereby creating a moving reference. At each time step we reference the density matrix from the simulations with an applied field to the density matrix at the corresponding time step in the simulation without an applied field. While all of the above has been framed in terms of TDDFT, the discussion applies equally well to time-dependent Hartree−Fock (TDHF).

All calculations were performed with a modified version of NWChem 6.5.[30] As with our previous studies,[8,29] the RT-TDDFT absorption spectra have been obtained from the imaginary part of the dipole polarizability, which is proportional to the Fourier transform of the dipole moment fluctuation. An exponential damping function has been applied to the dipole fluctuations before taking the Fourier transform in order to obtain smooth spectra. The decay constant of this damping function is related to the broadening in the resulting spectrum. The details, not described above, of our implementation of RT-TDDFT and LR-TDDFT gradients in NWChem can be found in the literature.[21,29]

3. RESULTS AND DISCUSSION

In order to demonstrate that meaningful information can be obtained with RT-TDDFT from an initially nonstationary density matrix, we have calculated ground-state absorption spectra of butadiene and an oligofluorene (H−(Fl)$_n$−H) with two fluorene units. Calculating the ground-state spectrum allows us to probe the consequences of starting from a nonstationary state without the additional complication of a different reference state as will be the case for ESA. For our nonstationary density matrix we utilized a superposition of atomic densities. The atomic superposition density (ASD) is the default initial guess density in NWChem and is a reasonable starting point for the self-consistent field (SCF) equations for most systems. This will be compared with the fully converged SCF density.

3.1. Nonstationary Ground State. For butadiene we made use of the B3LYP[31−33]/cc-pVDZ[34] optimized geometry and propagated the density using pure HF exchange (i.e., RT-TDHF) and the cc-pVDZ basis set. This geometry and level of

DOI: 10.1021/acs.jctc.5b00473
J. Chem. Theory Comput. 2015, 11, 4294−4303

theory combination were chosen to match with our ESA calculations presented below, which will be compared with previous QR-TDHF results using the same geometry and level of theory. The RT-TDHF simulations were propagated with a time-step of 0.1 atomic units (au) for 1000 au (~24 fs). Delta function electric fields were used to excite the molecule, with one simulation performed for a field applied along each of the Cartesian axes and an amplitude of 0.0001 au. An additional simulation without an applied field was performed for the simulation starting from the ASD in order to obtain a moving reference.

Figure 1 displays the ground state absorption spectrum calculated with the SCF density as well as the spectrum

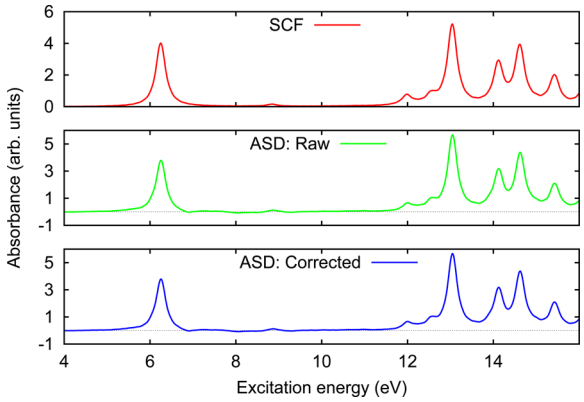

Figure 1. Comparison of ground state absorption spectrum of butadiene calculated at the HF/cc-pVDZ with a fully converged density (top) and an ASD before (middle) and after (bottom) correcting the dipole moments with the field-free reference. The spectra have been artificially broadened by 0.25 eV.

calculated by starting with the ASD. Remarkably, the spectrum calculated from the ASD without referencing the field-free propagation (middle plot in Figure 1) is in excellent agreement with the result from the SCF density. Indeed our correction derived from the field-free propagation has essentially no effect on the result (compare middle and bottom plots in Figure 1). While it would appear as if the ASD was somehow stationary in this case, we have confirmed by computing the commutator between the ASD and the initial Fock matrix that the initial density matrix is not stationary. The lack of any correction can be understood by noting that butadiene has no permanent dipole moment in its ground state.

A molecule without a permanent dipole moment has its charge distributed symmetrically. Since the equation of motion obeys the same symmetries as the molecule, there is nothing to cause an asymmetric charge distribution in the absence of any external perturbation such as an electric field. Therefore, from the perspective of the dipole, the initial density matrix appears stationary, and we see essentially no change in the dipole moment of butadiene during the field-free propagation.

This is shown explicitly in Figure 2 where we plot the evolution of the components of the dipole moment for the simulations. As can be seen in the second row of Figure 2, the components of the dipole moment do not change when there is no applied electric field. Artifacts still appear in the resulting spectrum due to the neglect of higher-order terms that couple the perturbation due to the electric field and the perturbation due to starting with a nonstationary density matrix. Fortunately, as our perturbative analysis suggests, these artifacts are generally small.

The H−$(Fl)_2$−H molecule *does* have a small permanent dipole moment in its ground state due to the fluorene units not lying in the same plane, and with it we can see the utility of our proposed correction. An optimized geometry for the first excited state of H−$(Fl)_2$−H, see Figure 9, was taken from the Supporting Information of ref 35. The molecule was optimized at the CAM-B3LYP[36]/6-31G[37] level, and our RT-TDDFT simulations were performed at the B3LYP/6-31G level using a time step of 0.2 au and a propagation length of 1000 au. As with butadiene, our choice of functional and basis set is for consistency with our ESA calculations presented below, which will be compared with previous QR-TDDFT results performed at the same level of theory. Again delta function electric fields with an amplitude of 0.001 au were used to excite the molecule, and our starting densities were the SCF density and the ASD.

Figure 3 shows the calculated ground state absorption spectra. Here, we can see that the spectrum calculated from the uncorrected ASD dipole moments does not even resemble an absorption spectrum. However, once we make use of our moving reference from the field-free propagation, we obtain excellent agreement with the result starting from the SCF density. Again some minor artifacts appear due to the neglect of the coupling between the nonstationary initial state and the electric field, but all the features of the spectrum are present and at the correct positions. For the orientation used in the simulation, the permanent dipole moment of H−$(Fl)_2$−H was aligned along the *z*-axis. We observe large oscillations of the z-component of the dipole in the field-free calculation (Figure 4). A dipole moment implies an unequal charge distribution. Since the initial state is not stationary, it seems reasonable to expect that the charge distribution is not stable and therefore could oscillate as the system propagates in time. After subtracting the dipole moment from the field-free simulation from the dipole moment from the simulation with an applied field, we are left with a dipole evolution that nearly matches the dipole from the SCF density perfectly. The x- and y-components of the permanent dipole moment are zero, and as with butadiene we see essentially no change in those components during the field-free propagation.

While it is quite remarkable that an accurate absorption spectrum can be obtained from an approximate guess of the ground-state density, a simple analogy with molecular vibrations helps to understand what is happening. The vibrational density of states of a molecule can be determined from the analysis of a molecular dynamics trajectory. While a normal mode calculation to determine the vibrations of a molecule would require that the molecule be at a stationary point on the potential energy surface, the molecular dynamics based approach only requires that the molecule be near the stationary point of interest. In the same way, because RT-TDDFT is propagating the density rather than just analyzing it at a single point, the method is able to obtain a meaningful spectrum even when the propagation is started away from a stationary point. This understanding of the ability of RT-TDDFT to obtain a meaningful result with a nonstationary initial state provides a key piece of validation as we explore ESA with RT-TDDFT.

3.2. H_2^+ and H_2 ESA. Having shown that our correction procedure can account for a nonstationary initial state, we will first consider two small systems to showcase our ESA approach. We have calculated the ground and ESA spectra for H_2^+ and H_2

DOI: 10.1021/acs.jctc.5b00473
J. Chem. Theory Comput. 2015, 11, 4294−4303

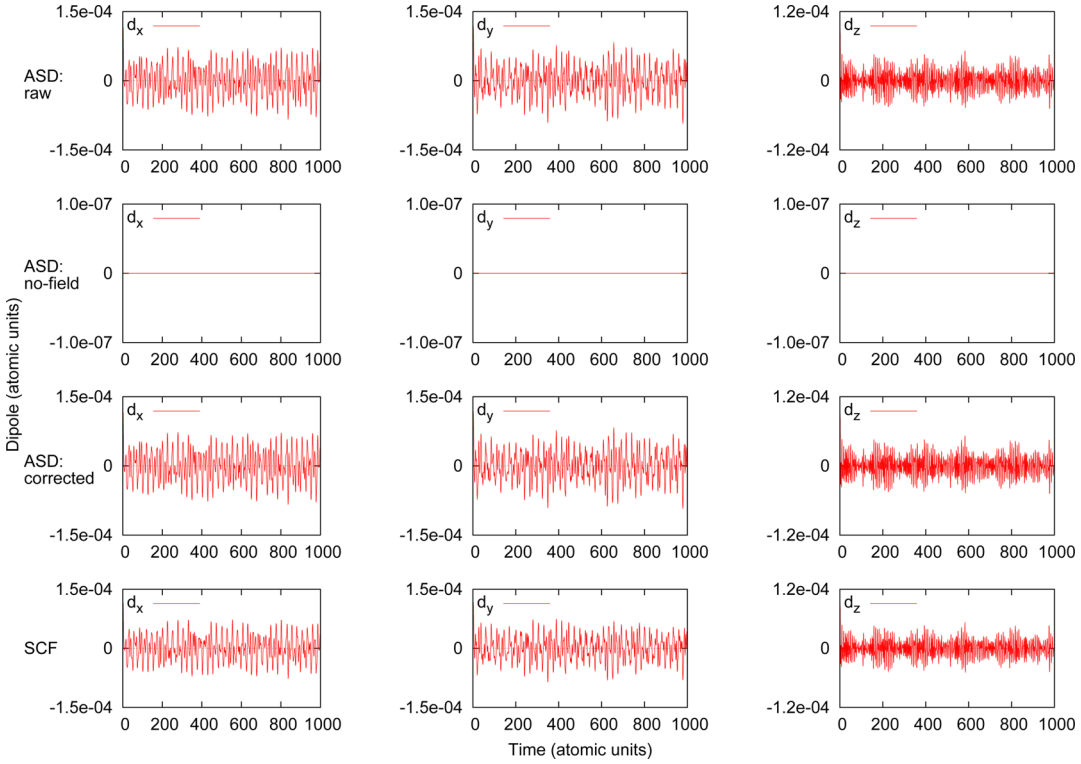

Figure 2. Dipole moments in atomic units for butadiene calculated with HF/cc-pVDZ for an atomic superposition density (rows 1−3) and a fully converged (bottom row) ground-state density. The top row gives the dipole moments from the simulations with an applied electric field. The second row gives the dipoles from the simulation with no applied field. The third row gives the corrected dipoles, obtained by subtracting the dipoles obtained from the field-free simulation from the dipoles obtained from the simulations with applied field. The bottom row gives the dipoles obtained from starting from a fully converged SCF density. The columns are the *x*, *y*, and *z* Cartesian components.

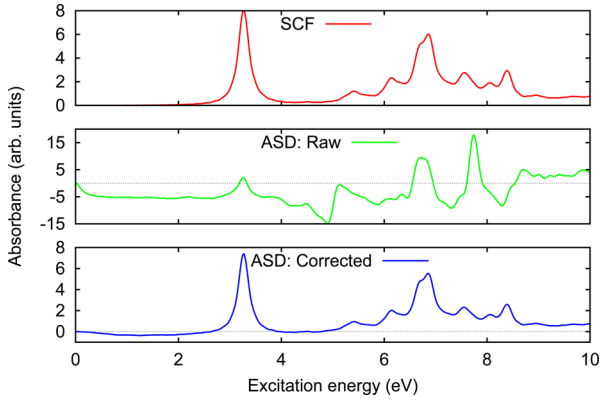

Figure 3. Comparison of ground state absorption spectrum of H−$(Fl)_2$−H calculated at the B3LYP/6-31G with a fully converged density (top) and an ASD before (middle) and after (bottom) correcting the dipole moments with the field-free reference. The spectra have been artificially broadened by 0.25 eV.

via RT-TDHF with the 6-31G basis set. This basis set was chosen so that there would be the possibility for both emission and absorption features in the ESA spectra, while at the same time keeping the number of states limited in order to aid in interpretation of the spectra. We optimized the geometry of both molecules in their ground states with HF/6-31G. RT-TDHF simulations with a time step of 0.1 au and a propagation length of 1000 au were run for each molecule. A delta function electric field was applied along the molecular axis with a maximum amplitude of 0.0001 au.

For the case of H_2^+, HF is an exact theory and allows an excellent proof-of-principle for our method. Shown in the top panel of Figure 5 are the ground and ESA spectra for H_2^+. Since our approach for ESA calculates the linear response of the excited state, it is natural to expect a response that corresponds to emission from the excited state back to the ground state. Indeed this is seen in the ESA spectrum for H_2^+. Additionally, since HF is exact for the one-electron case, the negative feature in the ESA spectrum has the same absolute intensity and is located at the same energy as the positive feature in the ground state spectrum. There is an additional absorption in the excited state spectrum that corresponds to excitation from the first excited state to the second excited state. This calculation serves as proof that emission is a natural part of our approach to obtaining the ESA spectrum and propagating an initially excited state with an exact functional yields the expected spectrum. In general though, we will be working with approximate methods.

Turning to the spectra for H_2, HF is no longer an exact theory; therefore, the exact correspondence between the ground and excited state spectra is lost. However, for the energy range considered, there should be three possible transitions in the ESA spectrum, as inferred from the results of a ground state LR-TDHF calculation: a transition back to the ground state, a transition of the second electron to the same orbital as the initially excited electron to form the doubly excited state, and a transition of the excited electron to a higher lying state. This is precisely what is seen in the excited state spectrum; there are two positive features corresponding to the two possible absorptions and a negative feature corresponding to the transition back to the ground state. As can be seen, the calculated emission occurs at a lower energy and is far less

DOI: 10.1021/acs.jctc.5b00473
J. Chem. Theory Comput. 2015, 11, 4294−4303

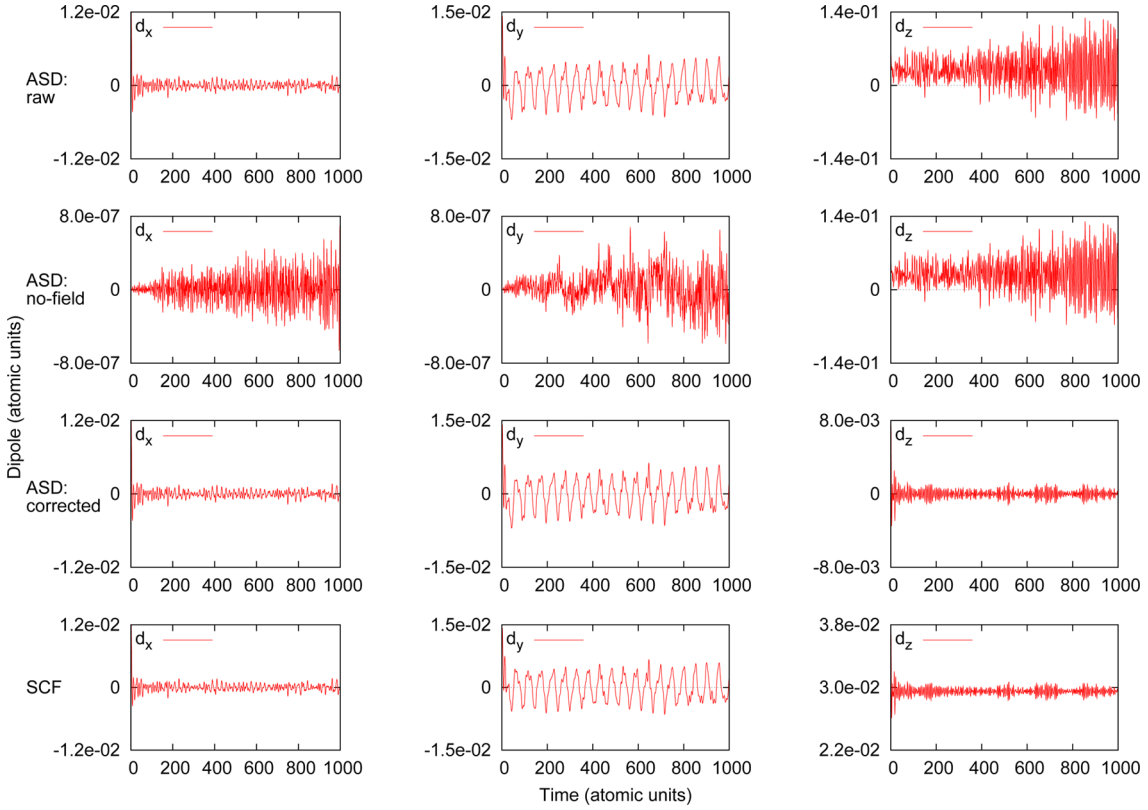

Figure 4. Dipole moments in atomic units for H−(Fl)$_2$−H calculated with B3LYP/6-31G for an atomic superposition density (rows 1−3) and a fully converged (bottom row) ground-state density. The layout is the same as in Figure 2.

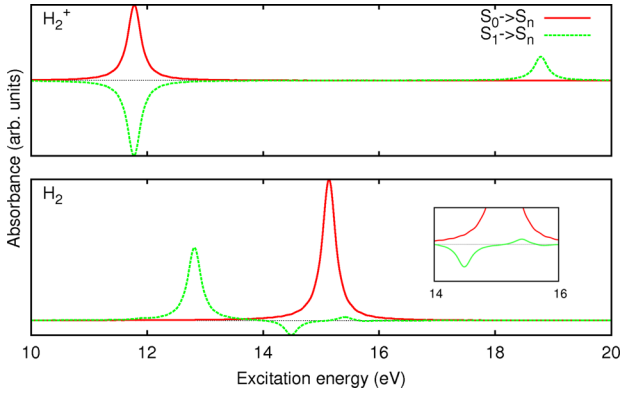

Figure 5. Ground (solid line) and excited state (broken line) absorption spectra for H_2^+ (top) and H_2 (bottom) calculated via RT-TDHF with the 6-31G basis set. Inset on the bottom plot is a closer look at the peaks in the ESA spectrum between 14 and 16 eV. For H_2^+ the excited state was obtained by solving the SCF equations with the constraint that the orbital with the second lowest energy be populated. The excited state for H_2 was obtained through LR-TDHF.

intense than the predicted absorption out of the ground state. We attribute these discrepancies to the change of reference between the ground and excited state and the use of a ground state exchange-correlation functional for the propagation of the excited state density.

To corroborate the assignment of the negative feature, we have calculated the transition density (ρ_ω) corresponding to the negative peak by taking the negative of the imaginary part of the Fourier transform of the time-dependent density fluctuation (δn) at that frequency[38]

$$\rho_\omega(\mathbf{r}) \propto -Im \int_{-\infty}^{\infty} dt\ \exp^{-i\omega t}[\delta n(\mathbf{r}, t)] \tag{7}$$

$$\delta n(\mathbf{r}, t) = n(\mathbf{r}, t) - \tilde{n}(\mathbf{r}, t) \tag{8}$$

where $n(\mathbf{r},t)$ is the density from the simulation with an applied field, and $\tilde{n}(\mathbf{r},t)$ is the density from the simulation without an applied field. This is compared with the transition density calculated from LR-TDHF for the ground-to-excited state transition (Figure 6). While the agreement between the densities is not perfect, there are strong qualitative similarities.

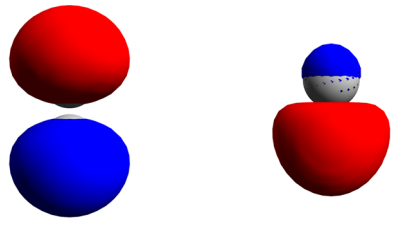

(a) LR-TDHF excitation (b) RT-TDHF emission

Figure 6. Transition densities for H_2 calculated from LR-TDHF for the first singlet transition and from RT-TDHF for the negative feature in the bottom panel of Figure 5. The RT-TDHF transition density was calculated via eqs 7 and 8.[38]

We note that there is a potential for ambiguity in our calculated ESA spectra. As seen with the ground state calculations starting from a nonstationary initial state, some artifacts may appear in the resulting spectrum since our correction procedure is only accurate to first order. While these artifacts generally appear to be small, a low intensity transition

DOI: 10.1021/acs.jctc.5b00473
J. Chem. Theory Comput. 2015, 11, 4294−4303

in the spectrum could be obscured by or mistaken for an artifact.

3.3. Butadiene ESA. Cronstrand et al.[6] have previously utilized QR-TDHF to calculate the ESA spectrum of butadiene. This provides us with an opportunity to test our RT-TDDFT based approach against QR-TDDFT. The calculations were based on the B3LYP/cc-pVDZ optimized, ground-state geometries, and the RT-TDDFT calculations were performed with pure HF exchange (i.e., RT-TDHF) and the cc-pVDZ and cc-pVTZ basis sets:[34] the same geometry and levels of theory used in the QR-TDHF calculations.

We note that our intention here is comparison with QR-TDHF and not to obtain a very accurate representation of the electronic structure of butadiene. The number of low-lying excited states with Rydberg and double-excitation character make accurate representation of the electronic structure of butadiene a challenge in and of itself. The question of how well our method would be able to address states with significant double-excitation character is intriguing as certain double excitations from the ground state would only be single excitations from an excited state. We plan on specifically addressing this question in a future study and for now focus on the comparison with QR-TDHF. Additionally, since there are no experimental references for the ESA spectrum of butadiene, we are only comparing with QR-TDHF, but we are not suggesting that QR-TDHF is the inherently more accurate method. Since the two approaches should agree in the limit of an exact treatment of the electronic structure though, it is reasonable to expect that they should give similar results with an approximate treatment of the electronic structure. The RT-TDDFT simulations used a time-step of 0.1 au and were propagated for 1000 au.

Figure 7 shows the ESA spectra of butadiene calculated with RT-TDHF and QR-TDHF, respectively. The RT-TDHF

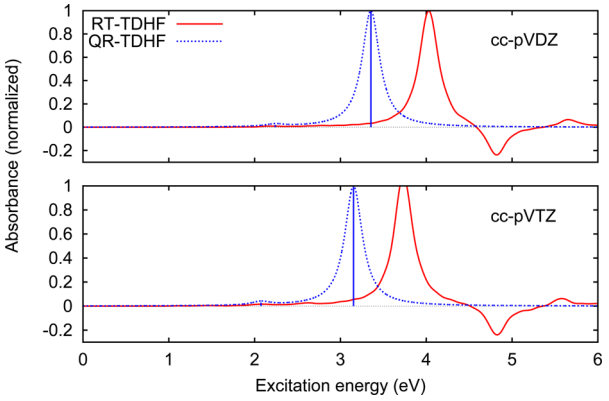

Figure 7. Comparison of excited state absorption spectra of butadiene calculated at the HF/cc-pVDZ (top) and HF/cc-pVTZ (bottom) levels with RT-TDHF (solid curve) and QR-TDHF (broken curve/sticks). The QR-TDHF results have been digitized from ref 6. The spectra have been artifically broadened by 0.25 eV.

results show good qualitative agreement with the QR-TDHF results of Cronstrand et al.[6] Note the QR-TDHF results are only for excitations to the first 7 excited states of A_g symmetry, while our RT-TDHF results cover all transitions out of the first excited state. Due to the difference in reference state, RT-TDHF predicts that the main peak occurs about 0.5 eV higher in energy as compared to QR-TDHF. Around 4.8 eV there is a negative feature, which we attribute to emission back to the ground state. We have again calculated the transition density for this feature and compared with that from LR-TDHF. This is shown in Figure 8, and the similarity between the transition

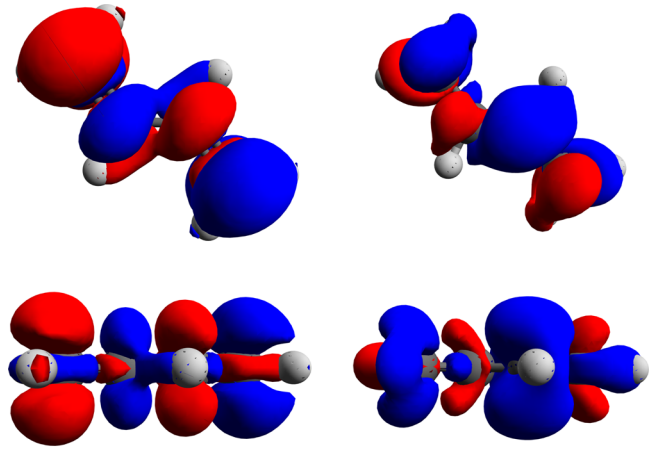

(a) LR-TDHF excitation (b) RT-TDHF emission

Figure 8. Transition densities of butadiene at the HF/cc-pVDZ level calculated from LR-TDHF for the first singlet transition and from RT-TDHF for the negative feature in the top panel of Figure 7. The RT-TDHF transition density was calculated via eqs 7 and 8.[38]

densities adds confidence to our assignment. The emission energies are underestimated by about 1.4 eV as compared to ground-to-excited state transition energies predicted by LR-TDHF (6.25 and 6.10 eV for cc-pVDZ and cc-pVTZ, respectively). Again, we rationalize this difference to be due to the change in reference state and the use of ground state exchange-correlation functionals for the simulation of the response of the excited state.

3.4. Oligofluorene ESA. As a final illustration of our new approach we have calculated the ESA of a pair of oligofluorenes (H−(Fl)$_n$−H). These molecules allow us to compare our results to both QR-TDDFT[35] and experiment.[39] We begin with the comparison to QR-TDDFT. Following the work of Ling et al.,[35] we performed calculations using the B3LYP and CAM-B3LYP functionals with the 6-31G basis set. Optimized geometries for the first excited state of oligomers with two and three fluorene units (H−(Fl)$_2$−H and H−(Fl)$_3$−H), see Figure 9, were taken from the Supporting Information of ref 35. Fast vibrational relaxation was observed in the experiments of Hayes and Silva,[39] indicating that the excited state geometry is most relevant for comparion with the experimental ESA spectra.

The RT-TDDFT equations were integrated with a time step of 0.2 au for 1000 au with a delta function field of amplitude 0.001 au applied at the beginning. Figure 10 shows the ESA calculated with QR-TDDFT and our RT-TDDFT approach, as well as the positions of the experimentally measured absorption maxima. Similar to the case of butadiene, the RT-TDDFT result predicts a larger excitation energy for the main transition in H−(Fl)$_2$−H by about 0.6 eV as compared to the QR-TDDFT result. However, for H−(Fl)$_3$−H, the two methods are within 0.2 eV of each other. Again we observe negative features that we are assigning as stimulated emission. These are underestimated for both H−(Fl)$_2$−H and H−(Fl)$_3$−H, though the discrepancy is smaller than for butadiene; the ground-to-excited state transition energies are 3.58 eV (H−(Fl)$_2$−H) and

DOI: 10.1021/acs.jctc.5b00473
J. Chem. Theory Comput. 2015, 11, 4294−4303

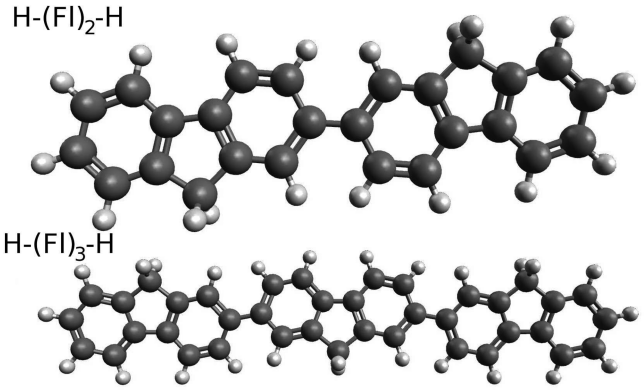

Figure 9. Excited state optimized geometries of the H−$(Fl)_2$−H and H−$(Fl)_3$−H molecules. The structures were rendered with Avogadro.[40]

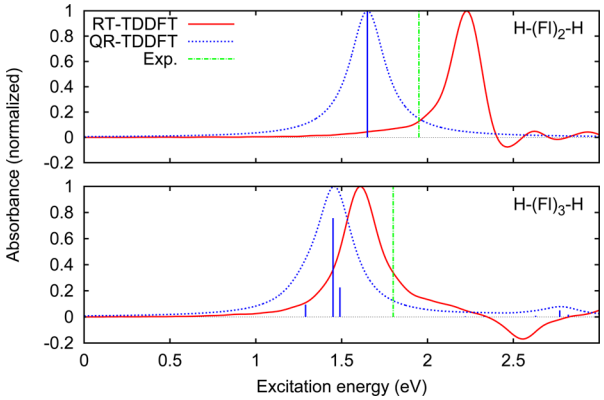

Figure 10. Excited state absorption spectra calculated with RT-TDDFT (solid curve) and QR-TDDFT (broken curve/sticks) at the CAM-B3LYP/6-31G level of theory. The QR-TDDFT results were taken from the Supporting Information of ref 35. The curves were artificially broadened by 0.25 eV. The positions of experimentally measured absorption maxima[39] are indicated by the dot-dash vertical lines.

3.40 eV (H−$(Fl)_3$−H). Figure 10 demonstrates one of the difficulties in assigning the negative features to emission. While for butadiene and H−$(Fl)_3$−H, the negative features that we are assigning to emissions are distinct peaks, the negative feature in H−$(Fl)_2$−H that we are calling an emission is the first negative feature in a ripple pattern after the main absorption. We make this assignment based on correspondence between the features in the H−$(Fl)_3$−H and H−$(Fl)_2$−H spectra. However, given that in general artifacts appear in our simulated results and the discrepancies between the ground state absorption energies and excited state emission energies, there is ambiguity in the assignments.

In the article by Ling et al.[35] the authors reported that B3LYP severely underestimated the ESA, giving a peak more than 1 eV lower in energy. Ling et al. suggested that this could be due to the well-known failure of TDDFT to properly describe charge transfer excitations. We performed our own simulation of the ESA spectra of H−$(Fl)_2$−H and H−$(Fl)_3$−H using B3LYP/6-31G with our RT-TDDFT approach, and the results are displayed in Figure 11, along with our CAM-B3LYP results for comparison. As can be seen, B3LYP provides similar performance to CAM-B3LYP as far as peak positions are concerned. The results for H−$(Fl)_2$−H do show a large

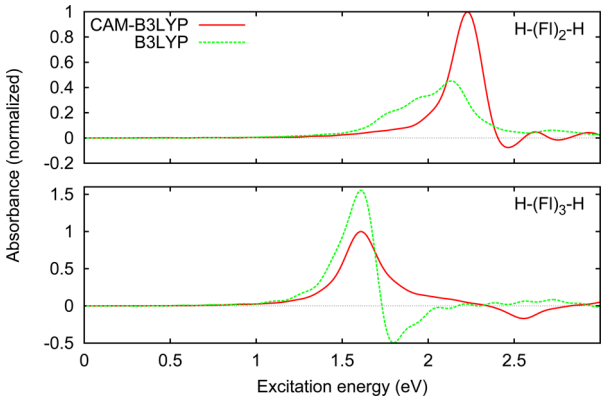

Figure 11. Excited state absorption spectra calculated with RT-TDDFT using the 6-31G basis set and either the CAM-B3LYP (solid curve) or B3LYP (broken curve) functional. The curves were artificially broadened by 0.25 eV and normalized to the CAM-B3LYP result.

difference in the intensity of the absorption however. The reason for this is alluded to in the results for H−$(Fl)_3$−H: stimulated emission and absorption overlap leading to decreased intensity. The ground-to-excited transition for H−$(Fl)_2$−H with the B3LYP functional is predicted to be 3.27 eV, which when combined with the ∼1 eV by which our method seems to underestimate emissions suggests that the emission would be predicted to occur right where the absorption peak is located. Running a longer simulation to increase the spectral resolution would help to distinguish between the transitions and reveal the true intensities of each. While the overlapping of an emission and an absorption is certainly an issue with our RT-TDDFT approach, we note that QR-TDDFT is not without its own issues.

Specifically, QR-TDDFT has an incorrect pole structure leading to spurious resonances when the energy difference between two excited states is equal to the energy difference between the ground state and another state.[41−45] It is possible that QR for spin-flip TDDFT does not suffer from these spurious poles.[44]

The large difference between the performance of the CAM-B3LYP and B3LYP functionals with QR-TDDFT versus the close performance of the functionals with RT-TDDFT is intriguing. We postulate two possibilities for the difference in results. First, if the failure of B3LYP in the QR-TDDFT calculation is due to an artificially low lying charge transfer state, then it is possible that by changing our reference state from the ground state to the excited state in the RT-TDDFT simulation, we managed to remove the offending state. What was a charge transfer state from the ground state may not be as much of a charge transfer state from the excited state. The second possibility may be related to the higher derivatives of the B3LYP functional. It has been shown before that even when a functional predicts reasonable exchange-correlation energies, the corresponding potentials may not resemble the true potentials.[46] If the first derivative of the exchange-correlation functional is already questionable, then the reliability of higher derivatives cannot be above suspicion. Indeed, a study of frequency dependent hyperpolarizabilities found that the quality of the predicted hyperpolarizabilities was sensitive to the asymptotic behavior of the exchange-correlation potential.[47] While QR-TDDFT would require third derivatives of the exchange-correlation energy for the calculation of transition

DOI: 10.1021/acs.jctc.5b00473
J. Chem. Theory Comput. 2015, 11, 4294−4303

moments, our RT-TDDFT approach only requires third derivatives for obtaining the initial density matrix. The propagation depends only on the exchange-correlation potential (first derivative of the energy). As we have demonstrated above, RT-TDDFT is not overly sensitive to the initial density matrix.

Turning to the comparison with experiment in Table 1, we have collected the positions of the peak maxima for the various calculations and the experimental measurements from ref 39. The experiments were performed with two and three unit oligomers of dihexylfluorene, where two *n*-hexyl chains are attached to the bridging carbons. The low-lying excited states involve transitions between the π-electrons of the main fluorene units; therefore, the hexyl chains have a minimal effect on these states, and a valid comparison can be made between the molecules used in the calculations and those used in the experiment for the energy range considered. In addition to the calculations already presented, we have also performed RT-TDDFT simulations with the B3LYP functional and a modified version of the Def2-SVPD basis set,[48] which we refer to as Def2-SVP(D). Our modification of the basis consists of simply removing the diffuse functions on the hydrogen atoms; all other aspects were left unchanged. The larger basis set produced ESA curves of the same shape as the smaller basis set. For H−$(Fl)_2$−H, our CAM-B3LYP RT-TDDFT value overestimates the excitation energy by the same amount by which the QR-TDDFT value underestimates it. For H−$(Fl)_3$−H, both methods underestimate the peak position, but the RT-TDDFT result is in better agreement. There is some uncertainty in the B3LYP RT-TDDFT values given the amount of overlap between emission and absorption. If the energies extracted from the simulation are accurate, then it appears B3LYP offers a slight improvement over CAM-B3LYP, at least for the smaller molecule. Going to a larger basis set marginally decreases the excitation energy for both molecules.

Table 1. Position of Peak Maximum in Excited State Absorption Spectra[a]

molecule	QR-TDDFT	RT-TDDFT	expt
H−$(Fl)_2$−H	1.65	2.23 (2.14/2.07)	1.95
H−$(Fl)_3$−H	1.46	1.60 (1.60/1.57)	1.80

[a]The calculated values are at the CAM-B3LYP/6-31G. The B3LYP/6-31G and B3LYP/Def2-SVP(D) results from the RT-TDDFT simulation are given in parentheses (6-31G/Def2). All energies are given in eV.

4. CONCLUSIONS

We have proposed a new method for obtaining excited state absorption (ESA) spectra from RT-TDDFT. By starting our RT-TDDFT propagation with the excited-state density obtained from a LR-TDDFT gradients calculation, we are able to obtain the response of the excited state to an external field. Due to exchange-correlation kernel approximations, our initial density matrix is not stationary. We have demonstrated the remarkable ability of RT-TDDFT to obtain meaningful and accurate spectra starting from a nonstationary state by first exploring ground state absorption before considering ESA. Our calculated excitation energies from the excited state are in reasonable agreement with QR-TDDFT and experiment. At the same time the emission energies are consistently underestimated by about 1 eV, a result that is not fully understood at this point. Additionally, there is some ambiguity in the assignment of emissions given that artifacts are not completely eliminated by our correction procedure.

The success of the method is encouraging in light of the work of Elliot and Maitra,[23] where they found that propagating initially excited states with state-of-the-art density functional approximations results in substantial errors. In particular they saw significant deviations in the time evolution of the dipole moment, which is of course directly related to the absorption spectrum. We rationalize that our success may be related to system size. Elliot and Maitra performed calculations on models of two and four electron systems. It is reasonable to expect that the density of the excited state for small systems does not resemble the density of the ground state. As such it is reasonable to conclude that a ground state density functional approximation will do a poor job of describing the dynamics of the excited state. On the other hand, as the system gets larger, it is more likely that the density of the excited state will resemble that of the ground state. By the same reasoning, ground state density functional approximations will be more likely to be able to accurately capture the dynamics of the excited state. There is some support for this line of thinking in the oligofluorene results as the calculated results for the larger molecule were in better agreement with experiment. Being based on RT-TDDFT, our new approach is intended for large molecular and materials systems where it can become more efficient to calculate the absorption spectrum by RT-TDDFT rather than LR-TDDFT/QR-TDDFT.

Beyond being a method for the calculation of ESA, our new approach could be a useful tool for the development of advanced density functional approximations. Currently we obtain a different set of response frequencies from propagating the excited-state density than would be expected based upon LR- or QR-TDDFT. In an exact treatment of the electronic structure, there should be a single, consistent set of transition energies, as was the case for H_2^+ (Figure 5). This is essentially the same condition on the exchange-correlation kernel that was recently proposed by Fuks et al.[49] in the context of resonant excitations within RT-TDDFT.

A. DEVIATION FROM IDEMPOTENCY

For an idempotent density matrix in a molecular orbital basis

$$\tilde{\mathbf{P}}'^2 - \tilde{\mathbf{P}}' = \mathbf{0} \tag{9}$$

where $\mathbf{0}$ is a zero matrix and $\tilde{\mathbf{P}}' = \frac{1}{2}\mathbf{P}'$. To quantify the deviation from idempotency of the excited state density matrices used in

Table 2. Frobenius Norm of the Difference between the Excited State Density Matrix and Square of the Excited State Density Matrix

system	level of theory	norm
H_2^+	HF/6-31G	0.000
H_2	HF/6-31G	0.289
butadiene	cc-pVDZ	0.441
	cc-pVTZ	0.629
H−$(Fl)_2$−H	CAM-B3LYP/6-31G	0.430
	B3LYP/6-31G	0.430
	B3LYP/Def2-SVP(D)	0.748
H−$(Fl)_3$−H	CAM-B3LYP/6-31G	0.543
	B3LYP/6-31G	0.526
	B3LYP/Def2-SVP(D)	0.749

DOI: 10.1021/acs.jctc.5b00473
J. Chem. Theory Comput. 2015, 11, 4294−4303

the current study, we have calculated the Frobenius norm of the difference in eq 9

$$\frac{\|\tilde{\mathbf{P}}'^2 - \tilde{\mathbf{P}}'\|}{N^2} = \frac{1}{N^2}\left[\sum_{i,j} |\tilde{\mathbf{P}}'^2 - \tilde{\mathbf{P}}'|_{ij}^2\right]^{1/2} \quad (10)$$

where N is the number of basis functions. The resulting values for each of the excited state density matrices used in the current study are given in Table 2. The norm was conserved during the propagation, indicating that we have stable, unitary dynamics for the density matrix.

AUTHOR INFORMATION

Corresponding Author

*E-mail: niri.govind@pnnl.gov.

Notes

The authors declare no competing financial interest.

ACKNOWLEDGMENTS

S.A.F. and N.G. thank Dr. Patrick El-Khoury for useful discussions. This work was supported by the U.S. Department of Energy, Office of Science, Office of Advanced Scientific Computing Research, Scientific Discovery through Advanced Computing (SciDAC) program under Award Numbers DE-SC0008666 (C.J.C.) and KC030102062653 (S.A.F., N.G.). The research was performed using EMSL, a DOE Office of Science User Facility sponsored by the Office of Biological and Environmental Research and located at the Pacific Northwest National Laboratory (PNNL). PNNL is operated by Battelle Memorial Institute for the United States Department of Energy under DOE contract number DE-AC05-76RL1830. The research also benefited from resources provided by the National Energy Research Scientific Computing Center (NERSC), a DOE Office of Science User Facility supported by the Office of Science of the U.S. Department of Energy under Contract No. DE-AC02-05CH11231 and resources provided by PNNL Institutional Computing (PIC).

REFERENCES

(1) Berera, R.; van Grondelle, R.; Kennis, J. T. M. *Photosynth. Res.* **2009**, *101*, 105−118.
(2) Jailaubekov, A. E.; Willard, A. P.; Tritsch, J. R.; Chan, W.-L.; Sai, N.; Gearba, R.; Kaake, L. G.; Williams, K. J.; Leung, K.; Rossky, P. J.; Zhu, X.-Y. *Nat. Mater.* **2013**, *12*, 66−73.
(3) Bellier, Q.; Makarov, N. S.; Bouit, P.-A.; Rigaut, S.; Kamada, K.; Feneyrou, P.; Berginc, G.; Maury, O.; Perry, J. W.; Andraud, C. *Phys. Chem. Chem. Phys.* **2012**, *14*, 15299−15307.
(4) Spangler, C. W. *J. Mater. Chem.* **1999**, *9*, 2013−2020.
(5) Cronstrand, P.; Christiansen, O.; Norman, P.; Ågren, H. *Phys. Chem. Chem. Phys.* **2000**, *2*, 5357−5363.
(6) Cronstrand, P.; Christiansen, O.; Norman, P.; Ågren, H. *Phys. Chem. Chem. Phys.* **2001**, *3*, 2567−2575.
(7) Wang, Y.; Lopata, K.; Chambers, S. A.; Govind, N.; Sushko, P. V. *J. Phys. Chem. C* **2013**, *117*, 25504−25512.
(8) Tussupbayev, S.; Govind, N.; Lopata, K.; Cramer, C. J. *J. Chem. Theory Comput.* **2015**, *11*, 1102−1109.
(9) De Giovannini, U.; Brunetto, G.; Castro, A.; Walkenhorst, J.; Rubio, A. *ChemPhysChem* **2013**, *14*, 1363−1376.
(10) Ruggenthaler, M.; Bauer, D. *Phys. Rev. Lett.* **2009**, *102*, 233001.
(11) Fuks, J. I.; Helbig, N.; Tokatly, I. V.; Rubio, A. *Phys. Rev. B: Condens. Matter Mater. Phys.* **2011**, *84*, 075107.
(12) Raghunathan, S.; Nest, M. *J. Chem. Theory Comput.* **2011**, *7*, 2492−2497.
(13) Ramakrishnan, R.; Nest, M. *Phys. Rev. A: At., Mol., Opt. Phys.* **2012**, *85*, 054501.
(14) Raghunathan, S.; Nest, M. *J. Chem. Phys.* **2012**, *136*, 064104.
(15) Raghunathan, S.; Nest, M. *J. Chem. Theory Comput.* **2012**, *8*, 806−809.
(16) Habenicht, B. F.; Tani, N. P.; Provorse, M. R.; Isborn, C. M. *J. Chem. Phys.* **2014**, *141*, 184112.
(17) Burke, K.; Werschnik, J.; Gross, E. K. U. *J. Chem. Phys.* **2005**, *123*, 062206.
(18) Li, X.; Tully, J. C. *Chem. Phys. Lett.* **2007**, *439*, 199−203.
(19) Moss, C. L.; Isborn, C. M.; Li, X. *Phys. Rev. A: At., Mol., Opt. Phys.* **2009**, *80*, 024503.
(20) Furche, F.; Ahlrichs, R. *J. Chem. Phys.* **2002**, *117*, 7433−7447.
(21) Silverstein, D. W.; Govind, N.; van Dam, H. J. J.; Jensen, L. *J. Chem. Theory Comput.* **2013**, *9*, 5490.
(22) Marques, M. A.; Gross, E. K. U. *Annu. Rev. Phys. Chem.* **2004**, *55*, 427−455.
(23) Elliott, P.; Maitra, N. T. *Phys. Rev. A: At., Mol., Opt. Phys.* **2012**, *85*, 052510.
(24) Runge, E.; Gross, E. K. U. *Phys. Rev. Lett.* **1984**, *52*, 997−1000.
(25) Li, T.; Tong, P. *Phys. Rev. A: At., Mol., Opt. Phys.* **1985**, *31*, 1950−1951.
(26) Li, T.; Li, Y. *Phys. Rev. A: At., Mol., Opt. Phys.* **1985**, *31*, 3970−3971.
(27) van Leeuwen, R. *Phys. Rev. Lett.* **1999**, *82*, 3863−3866.
(28) Isborn, C. M.; Li, X. *J. Chem. Phys.* **2008**, *129*, 204107.
(29) Lopata, K.; Govind, N. *J. Chem. Theory Comput.* **2011**, *7*, 1344−1355.
(30) Valiev, M.; Bylaska, E. J.; Govind, N.; Kowalski, K.; Straatsma, T. P.; van Dam, H. J. J.; Wang, D.; Nieplocha, J.; Apra, E.; Windus, T. L.; de Jong, W. A. *Comput. Phys. Commun.* **2010**, *181*, 1477−1489.
(31) Becke, A. D. *J. Chem. Phys.* **1993**, *98*, 5648−5652.
(32) Lee, C. T.; Yang, W. T.; Parr, R. G. *Phys. Rev. B: Condens. Matter Mater. Phys.* **1988**, *37*, 785−789.
(33) Vosko, S. H.; Wilk, L.; Nusair, M. *Can. J. Phys.* **1980**, *58*, 1200−1211.
(34) Dunning, T. H., Jr. *J. Chem. Phys.* **1989**, *90*, 1007−1023.
(35) Ling, S.; Schumacher, S.; Galbraith, I.; Paterson, M. J. *J. Phys. Chem. C* **2013**, *117*, 6889−6895.
(36) Yanai, T.; Tew, D. P.; Handy, N. C. *Chem. Phys. Lett.* **2004**, *393*, 51−57.
(37) Hehre, W. J.; Ditchfield, R.; Pople, J. A. *J. Chem. Phys.* **1972**, *56*, 2257−2261.
(38) Hofmann, D.; Kümmel, S. *J. Chem. Phys.* **2012**, *137*, 064117.
(39) Hayes, S. C.; Silva, C. *J. Chem. Phys.* **2010**, *132*, 214510.
(40) Hanwell, M. D.; Curtis, D. E.; Lonie, D. C.; Vandermeersch, T.; Zurek, E.; Hutchinson, G. R. *J. Cheminf.* **2012**, *4*, 17.
(41) Dalgaard, E. *Phys. Rev. A: At., Mol., Opt. Phys.* **1982**, *26*, 42−52.
(42) Li, Z.; Liu, W. *J. Chem. Phys.* **2014**, *141*, 014110.
(43) Li, Z.; Suo, B.; Liu, W. *J. Chem. Phys.* **2014**, *141*, 244105.
(44) Zhang, X.; Herbert, J. M. *J. Chem. Phys.* **2015**, *142*, 064109.
(45) Ou, Q.; Bellchambers, G. D.; Furche, F.; Subotnik, J. E. *J. Chem. Phys.* **2015**, *142*, 064114.
(46) Filippi, C.; Umrigar, C. J.; Taut, M. *J. Chem. Phys.* **1994**, *100*, 1290−1296.
(47) van Gisbergen, S. J. A.; Snijders, J. G.; Baerends, E. J. *J. Chem. Phys.* **1998**, *109*, 10657−10668.
(48) Rappoport, D.; Furche, F. *J. Chem. Phys.* **2010**, *133*, 134105.
(49) Fuks, J. I.; Luo, K.; Sandoval, E. D.; Maitra, N. T. *Phys. Rev. Lett.* **2015**, *114*, 183002.

DOI: 10.1021/acs.jctc.5b00473
J. Chem. Theory Comput. 2015, 11, 4294−4303